



The nature inspired peptide [T20K]-kalata B1 induces anti-tumor effects in anaplastic large cell lymphoma

Judith Lind^{a,b,c}, Roland Hellinger^a, Petra Kudweis^b, Herwig P. Moll^a, Jasmin Gattringer^a, Kathrin Thell^a, Sophie Edtmayer^e, Christian W. Gruber^{a,*}, Dagmar Stoiber^{a,d,e,**}, Karoline Kollmann^{b,*}

^a Institute of Pharmacology, Center for Physiology and Pharmacology, Medical University of Vienna, Vienna, Austria

^b Institute of Pharmacology and Toxicology, University of Veterinary Medicine, Vienna, Austria

^c Division Molecular Oncology/Haematology, Karl Landsteiner University of Health Sciences, Krems an der Donau, Austria

^d Ludwig Boltzmann Institute for Cancer Research, Vienna, Austria

^e Division Pharmacology, Department Pharmacology, Physiology and Microbiology, Karl Landsteiner University of Health Sciences, Krems an der Donau, Austria

ARTICLE INFO

Keywords:

Circular peptide
ALCL
Natural product
Apoptosis
Leukemia

ABSTRACT

Ribosomally synthesized and post-translationally modified peptides, such as plant cyclotides, are a diverse group of natural products well known as templates in drug discovery and therapeutic lead development. The cyclotide kalata B1 (kB1) has previously been discovered as immunosuppressive agent on T-lymphocytes, and a synthetic version of this peptide, [T20K]kB1 (T20K), has been effective in reducing clinical symptoms, such as inflammation and demyelination, in a mouse model of multiple sclerosis. Based on its T-cell modulatory impact we studied the effects of T20K and several analogs on the proliferation of anaplastic large cell lymphoma (ALCL), a heterogeneous group of clinically aggressive diseases associated with poor prognosis. T20K, as a prototype drug candidate, induces apoptosis and a proliferation arrest in human lymphoma T-cell lines (SR786, Mac-2a and the Jurkat E6.1) in a concentration dependent fashion, at least partially via increased STAT5 and p53 signaling. In contrast to its effect on IL-2 signaling in lymphocytes, the cytokine levels are not altered in lymphoma cells. *In vivo* mouse experiments revealed a promising activity of T20K on these cancer cells including decreased tumor weight and increased apoptosis. This study opens novel avenues for developing cyclotide-based drug candidates for therapy of patients with ALCL.

1. Introduction

Anaplastic large cell lymphoma (ALCL) belongs to non-Hodgkin lymphomas (NHL) and forms a group of mature T-cell derived cancers characterized by large lymphoid cells frequently expressing high amounts of CD30 [1]. The disease is classified into anaplastic lymphoma kinase (ALK)-positive and ALK-negative ALCL [2]. ALK-positive ALCL is mainly affecting children and young adults while ALK-negative ALCL dominates in older patients from their fifties on [1]. Tumorigenesis in ALK-positive patients depends on ALK activation while its inhibition is key for therapeutic success [3]. Constitutive kinase activity in turn leads to activation of several signaling pathways, such as JAK/STAT, PI3K/AKT, MAPK and PLC γ , resulting in proliferation, prolonged tumor

cell survival, cytoskeletal rearrangements and cell migration [4–6].

Treatment of ALCL is difficult due to its genetic heterogeneity, especially for ALK-negative ALCL, which is rare and lacks clear clinical and genetic markers that can be used to guide chemotherapy. Standard treatment of ALCL comprises the CHOP chemotherapy-regimen. ALK-positive patients have a 5-year overall survival rate of 80%, while it is only 50% in ALK-negative ALCL patients [1–4]. This poor prediction and the fact that ALK kinase inhibitors can lead to severe side effects and numerous resistance mechanisms new treatment approaches are highly needed for ALK-positive and –negative ALCL.

As exemplified by today's chemotherapeutic drug repertoire – vincristine is an alkaloid originally isolated from the plant *Catharanthus roseus*; doxorubicin, a derivative of daunorubicin, first isolated from

* Corresponding authors.

** Corresponding author at: Institute of Pharmacology, Center for Physiology and Pharmacology, Medical University of Vienna, Vienna, Austria.

E-mail addresses: christian.w.gruber@meduniwien.ac.at (C.W. Gruber), dagmar.stoiber@kl.ac.at (D. Stoiber), karoline.kollmann@vetmeduni.ac.at (K. Kollmann).

¹ These authors contributed equally.

<https://doi.org/10.1016/j.bioph.2022.113486>

Received 19 May 2022; Received in revised form 18 July 2022; Accepted 27 July 2022

Available online 2 August 2022

0753-3322/© 2022 The Author(s). Published by Elsevier Masson SAS. This is an open access article under the CC BY license (<http://creativecommons.org/licenses/by/4.0/>).

actinobacteria of the genus *Streptomyces* – nature has been and still is a major source of bioactive compounds for drug discovery and development [7]. In recent years, ribosomally synthesized and post-translationally modified peptides, amongst them the so-called cyclotides [8], attracted attention due to their effects on T-lymphocytes and immunosuppressive activity [9]. Cyclotides are a combinatorial library of plant-derived circular peptides [10]. They consist of around 30 amino acids and their three-dimensional structure makes them remarkably stable against enzymatic, chemical and thermal degradation [11]. Their intrinsic biological activities include uterotonic [12,13], anti-tumor activity [14–16] and suppression of T-cell proliferation [9,17]. Cyclotides were originally isolated from the coffee family plant *Oldenlandia affinis* (Rubiaceae) [18], but have since been discovered in many flowering plant species, from violets (Violaceae), cucurbits (Cucurbitaceae), legumes (Fabaceae), nightshades (Solanaceae) and grasses (Poaceae) [18,19].

In an earlier study, the prototypic cyclotide kalata B1 (kB1) has been discovered to exhibit anti-proliferative effects on activated peripheral blood mononuclear cells (PBMCs) [9]. Synthesis and screening of several kB1 analogs revealed the cyclotide [T20K]kB1 (T20K) as lead compound in T-cell proliferation studies. T20K reduced the proliferative capacity of T-cells and decreased IL-2 expression [20]. This observation was verified *in vivo* using the experimental autoimmune encephalomyelitis mouse model for multiple sclerosis, an autoreactive T-lymphocyte disease, where the therapeutic effect of T20K was successfully demonstrated in comparison to the approved multiple sclerosis drug FTY720 [21]. In fact, this cyclotide has recently shown favorable safety and tolerability in a clinical phase I trial [22] and is considered for further development in a clinical phase II study.

Therefore, we hypothesized a suppressive function on other dysfunctional T-cell mediated diseases such as ALCL. To clarify the structure-activity relationship of the peptide, different active and inactive mutants of kalata B1 were generated and assessed for their immunosuppressive activity. We tested the effects of these peptides on proliferation and apoptosis of several human ALCL cell lines. Furthermore, we determined the influence on IL-2 production and how effective these peptides are in mouse models to ameliorate disease phenotype.

2. Materials and methods

2.1. Peptide synthesis and analytical chemistry

Peptides (Suppl. Table 1) were synthesized via solid phase peptide synthesis, followed by head-to-tail cyclization and oxidative folding as published earlier [20,21]. Peptides were purified via reversed-phase preparative high-performance liquid chromatography. Quality and purity of peptides was determined by analytical high-performance liquid chromatography and mass spectrometry [20,21,23].

2.2. Mice

NOD.Cg-Prkdcscid-II2rgtm1Wjl/SzJ mice were used for tumor transplantations. Mice were *s.c.* injected with 0.75×10^6 cells/flank of SR786 cells and monitored daily. Treatment started on the same day as the tumor cells were injected. Mice were treated three times per week with a dose of 1 mg/kg T20K in PBS *i.p.* or using PBS as negative control. Tumor formation was monitored over time and mice sacrificed after tumors had grown to a volume of $\leq 2 \text{ cm}^3$. Tumors were isolated and further analyzed for proliferation, apoptosis and cell cycle state using flow cytometric analysis, Western blot and qPCR as described below.

All procedures were approved by the institutional ethics and animal welfare committee and the national authority according to §§26ff. of Animal Experiments Act, Tierversuchsgesetz 2012 – TVG 2012. (BMBWF-68.205/0174-V/3b/2018; BMBWF-68.205/0106-V/3b/2019; BMBWF-68.205/0091-V/3b/2019).

2.3. Cell lines, cell culture and reagents

Human ALK-positive ALCL cell lines (Karpas 299, SU-DHL-1, SR786, SUP-M2), ALK-negative cell lines (Mac-1a and Mac-2a) and the T-cell leukemia cell lines HPB-ALL, Jurkat WT and Jurkat E6.1 as well as the Burkitt-lymphoma B-cell lines Ramos and Daudi were obtained from ATCC. All cell lines were routinely maintained in RPMI 1640 (Sigma-Aldrich, Germany) supplemented with 10% FBS (Capricorn Scientific, Germany), 2 mM L-glutamine, 100 U/ml penicillin and 100 µg/ml streptomycin (all Sigma-Aldrich) at 37 °C with 5% CO₂ atmosphere.

2.4. Cell viability assays

Cell viability was determined using the Cell Counting Kit-8 (CCK-8; Dojindo EU, Germany). In brief, 4×10^4 cells/well were seeded in 96 well plates, cultivated in RPMI 1640 media at 37 °C with 5% CO₂ and allowed to rest for 2 h prior to treatment with appropriate concentrations of cyclotides for 2–24 h. The water-soluble tetrazolium salt based CCK-8 solution was added and the plate further incubated for 4 h. The absorbance of the resulting formazon dye was recorded at 450 nm using a microplate reader (Tecan, Austria), reference wavelength 600 nm, and the viability presented as percentage of treated versus untreated cells. As positive control for apoptosis, camptothecin (CPT) (30 µM) and/or cyclosporine A (CsA) (0.8 µM), and for necrosis, Triton-X 100 (0.5%) (all Sigma-Aldrich) were used.

2.5. Annexin V/7-AAD staining and cell cycle analysis

For Annexin V/7AAD staining and cell cycle analysis, 5×10^5 cells/well were seeded in 24 well plates in RPMI 1640 medium. The cells were allowed to rest for 2 h prior to treatment with cyclotides in indicated concentrations for 2–24 h and harvested for flow cytometry analysis. The percentage of apoptotic cells was determined by using the Annexin V-FITC apoptosis detection kit (eBioscience, Austria) according to the manufacturer's instruction. After Annexin V staining, 7-AAD staining solution (eBioscience) was added. The cells were incubated in the dark, followed by flow cytometric analysis on a FACS Canto II (BD Bioscience), to detect the percentage of apoptotic and necrotic cells. For cell cycle analysis cells were incubated with propidium iodide (PI) staining solution (eBioscience) (20 µg/ml PI and 100 µg/ml RNase) in PI buffer (0.1% Na-citrate, 0.1% Triton-X) for 30 min at 37 °C and afterwards cell cycle status was determined by flow cytometry.

2.6. Proliferation assays

For determination of cell division and proliferation, cells were harvested, washed twice in RPMI 1640 media without fetal calf serum (FCS) and resuspended at 1×10^7 cells/ml. Cells were incubated for 10 min in 5 µM proliferation dye eFluor™ 670 (eBioscience) at 37 °C in pure media. The reaction was stopped by addition of RPMI 1640 media containing FCS. Afterwards cells were seeded in 48 well plates at a concentration of 1×10^5 cells/well, treated with appropriate concentrations of cyclotides and analyzed over time by flow cytometry measurement using FACS Canto II.

2.7. Phospho-gamma H2A.X staining

For phospho-gamma H2A.X staining, 3×10^5 cells/well were seeded in 48-well plates, allowed to rest for 2 h and treated with T20K (4 µM), [V10A]kB1 (4 µM) or cladribine (100–500 nM) as positive control for 24–48 h. Cells were harvested, fixed and permeabilized using Fix and Perm solution (Thermo Fisher, Austria) and after permeabilization incubated with phospho-gamma-H2A.X-AF488 (Cell Signaling, Germany) for 1 h at room temperature and subsequently analyzed via flow cytometry using a FACS Canto II.

2.8. IL-2 secretion analysis

Cells were cultured without or with pre-stimulation using activating mitogens interleukin (IL)-2 (2.5 ng/ml) or phorbol 12-myristate 13-acetate (PMA) (50 ng/ml) in combination with ionomycin (500 ng/ml) followed by treatment with cyclotide T20K (4 μ M) for 2–24 h. For stimulated cells media was afterwards replaced to remove any excess of stimulant and/or cyclotide and followed by re-stimulation with PMA and ionomycin and further cultivation for 72 h. Supernatant was harvested and used for IL-2 ELISA measurement (Thermo Fisher).

2.9. IL-2 surface receptor analysis

Cells were treated with indicated cyclotides for 24 h, harvested, washed with PBS and stained with allophycocyanin (APC)-labelled anti-human CD25 monoclonal antibody (mAb) (Biolegend) for 30 min on ice in the dark. Afterwards cells were washed twice, analyzed by flow cytometry measurement on a FACS Canto II and FACSDIVA software for evaluation (BD Biosciences).

2.10. Immunoblot analysis

Proteins were isolated using RIPA buffer supplemented with a protease inhibitor cocktail (cOmplete™, Roche) by shaking 30 min and 20 min centrifugation at 13,000 rpm at 4 °C. Concentrations of the whole-cell lysates were measured colorimetric (Pierce™ BCA Protein Assay Kit, Thermo Scientific) on EnSpire® Multimode Plate Reader (Perkin Elmer). Protein lysates were incubated at 95 °C with Laemmli Buffer before loading onto the 10 or 12% sodium dodecyl sulphate polyacrylamide (SDS-PAGE) gel. Separated proteins were transferred to methanol activated Immobilon®-P Polyvinylidene difluoride membrane (PVDF; Merck, Darmstadt, Germany) by overnight blotting with 0.2 mA followed by 0.4 mA for 5 h at 4 °C. Membranes were blocked with 5% BSA in Py-TBST buffer and incubated overnight with the primary antibodies in 3% BSA. Secondary antibodies were incubated 1 h at room temperature (RT). Chemiluminescence of the membranes was measured with the ChemiDoc™ Imaging System (Bio-Rad, Hercules, CA, USA) after incubation with 20X LumiGLO® Reagent and 20X Peroxide (Cell Signaling Technology, Danvers, MA, USA). The densitometric quantification of signals was performed with the Image Lab 5.2.1. Software (Bio-Rad, Berkeley, CA, USA).

Antibodies used in this study:

Target	Description/Company
p53	SC-6243 Santa Cruz
HSC70	SC-7298 Santa Cruz
Anti-mouse IgG HRP-linked	7076S Cell Signaling
Anti-rabbit IgG HRP-linked	7074S Cell Signaling

2.11. RNA isolation and quantitative real time PCR

RNA of pretreated cells was isolated using the Qiagen RNA isolation kit (Qiagen, Netherlands) according to the manufacturer's protocol and RNA concentration quantified using Nanodrop (Thermo Fisher). For cDNA synthesis 750–1000 ng RNA were used and processed with the iScript cDNA synthesis kit (Bio-Rad) according to the manual of the manufacturer. Expression of mRNA was quantified using the Bio-Rad-SSO Advanced Universal Sybr Green Supermix on the Bio-Rad-qPCR cycler CF96 real-time-system, C1000 touch Thermal cycler. The following primer (Microsynth AG) sequences were used:

BCL-2 forward: 5'-ATGTGTGGAGAGCGTCAACC-3',
BCL-2 reverse: 5'-TGAGCAGAGTCTTCAGACAGCC-3',

BCL-XL forward: 5'-GATCCCCATGGCAGCAGTAAAGCAAG-3',
BCL-XL reverse: 5'-CCCCATCCCGGAAGAGTTCATTCACT-3',
MCL-1 forward: 5'-CATTCTGATGCCACCTTCT-3',
MCL-1 reverse: 5'-TCGTAAGGACAAAACGGGAC-3',
STAT3 forward: 5'-ACATCAGTGGCAAGACCCAGATCC-3',
STAT3 reverse: 5'-ACCTGGGTCGGCTTCGGG-3',
STAT5A forward: 5'-GGCTCCCTATAACATGTACCC-3',
STAT5A reverse: 5'-AAGACTGTCCATTGGTCGGCG-3',
GAPDH forward: 5'-TCTCTCTGACTTCAACAGCG-3',
GAPDH reverse: 5'-ACCACCCTGTTGCTGTAGCC-3'.

2.12. Statistical analysis

Data are reported as mean values \pm SEM. Biochemical experiments were performed in triplicates and a minimum of three independent experiments was evaluated. Statistical analysis to determine group differences was done by unpaired Student t-test, One-way or Two-way ANOVA multiple test using GraphPad Prism software (Graphpad, San Diego, CA; <http://www.graphpad.com>). The p values are considered as follows: *p < .05; **p < .01; ***p < .001.

3. Results

In recent years, the discovery of the immunosuppressive and anti-proliferative effects of plant-derived cyclic peptides opened the door to explore their therapeutic application [17,20,21]. In particular, the promising effects of T20K in a mouse model of multiple sclerosis provided an opportunity for treatment of other immune cell-related disorders such as ALCL. In the current work we characterized kalata-type cyclotides (Fig. 1; Suppl. Table 1) regarding their effects on lymphoma, in particular several ALCL cell lines. Seven single or double point-mutated lysine or alanine analogs ([T8K]-, [V10A]-, [V10K]-, [G18K]-, [T20K]-, [N29K]- and [G1K, T20K]kB1; Suppl. Table 1) were chemically synthesized and tested for their impact on viability and proliferation of ALCL cells to gain insight on the structure of kalata-type peptides.

3.1. Cyclotides affect viability of ALCL cell lines

Using a water-soluble tetrazolium salt-based cytotoxicity assay (CCK-8) we tested the seven cyclotides for reactivity on human ALK-positive and -negative T-cell lines. The different cell lines were treated for 24 h with 2 and/or 4 μ M of cyclotides. These two concentrations are a consensus of the determined inhibitory concentration IC₅₀ of the lead compound T20K using freshly isolated PBMCs as well as of recently published reference data (Suppl. Fig. 1) [20].

Cyclotide analogs [G18K]-, [N29K]- and [G1K, T20K]kB1 or the peptide T20K significantly decreased cell survival of the ALK-positive ALCL cell line (SR786, Fig. 2A), ALK-negative cell line (Mac-2a, Fig. 2B), as well as the T-cell leukemia cell line (Jurkat E6.1, Fig. 2C). The inactive derivative [V10A]kB1 and the analogs [T8K]- and [V10K]kB1 had no effect on the viability of these cell lines. Active cyclotides, including [G18K]-, [N29K]- and [G1K, T20K]kB1, decreased cell survival in the SR786 between 0% and 83%, Mac-2a between 96% and 100% and Jurkat E6.1 between 32% and 99%. T20K as prototype peptide candidate exhibited a concentration dependent effect and suppressed cell survival by 20% in the SR786, 73% in the Mac-2a and 26% in the Jurkat E6.1 (at 2 μ M) and 47% in the SR786, 91% in the Mac-2a and 76% in the Jurkat E6.1 (4 μ M). Overall, T20K (at 4 μ M) had comparable significant effects on cell survival as its active analogs (p < .0001).

Moreover, the apoptotic and necrotic potential on ALK-positive (SR786, Karpas, SUD-HL-1, SUP-M2) and ALK-negative ALCL cell lines (Mac-1a, Mac-2a) of the different cyclotides was tested using Annexin V and 7-AAD-staining (Fig. 2D and Suppl. Fig. 2A and B). In conclusion, these experiments demonstrate an apoptotic and necrotic function of the

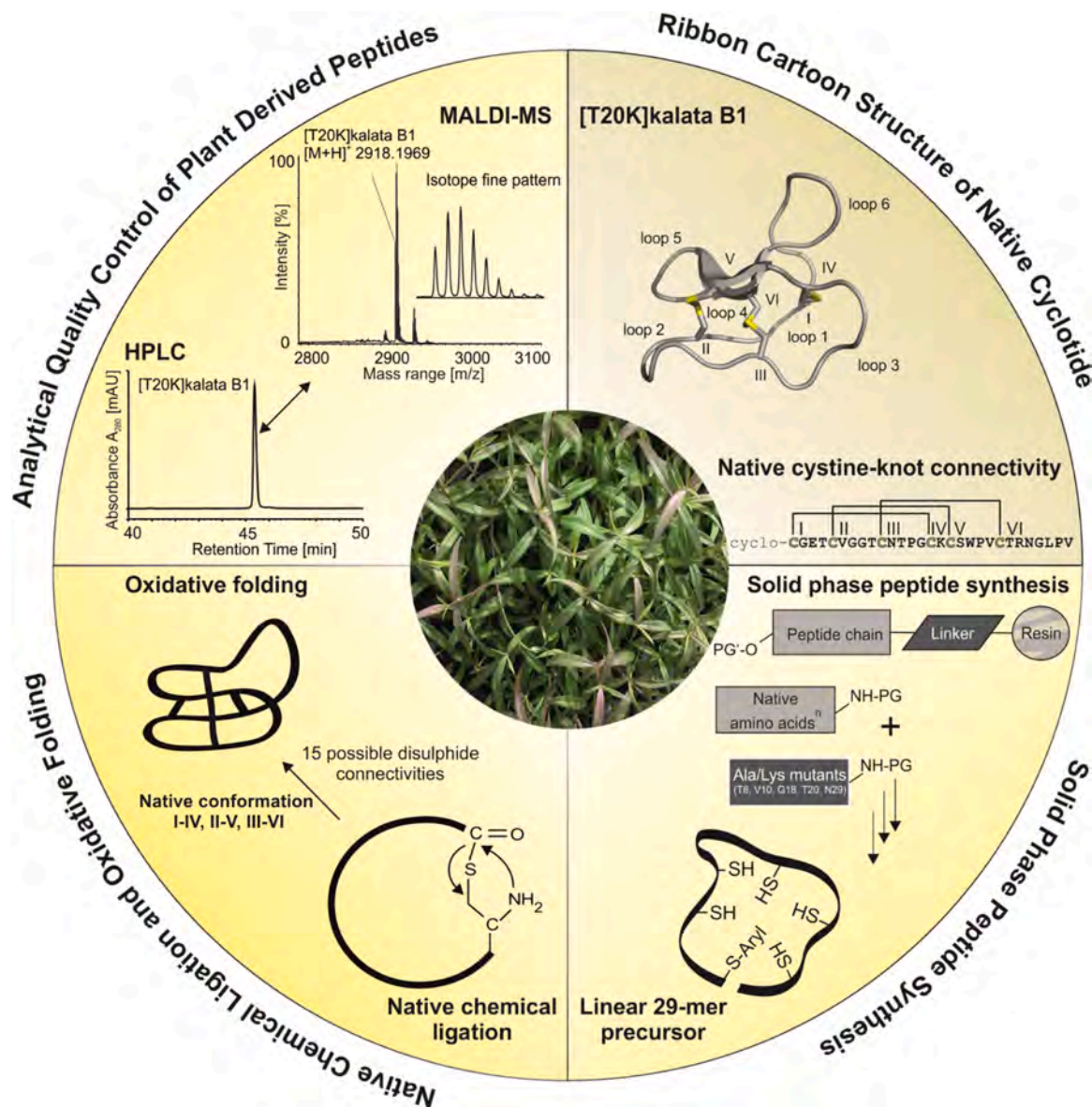


Fig. 1. Structure and synthesis of kalata-type cyclotides. Pie-shaped flow chart demonstrates the solid phase peptide synthesis of kalata-type cyclotides by example of T20K. The solid phase peptide synthesis used standard protocols for peptide elongation on a solid support modified by a thioester linker moiety. The fully elongated peptide is cleaved off the resin as a linear unprotected thioester peptide supporting the peptide cyclization (right, lower quarter). The cyclized peptide is generated with a ‘native chemical ligation’, a reaction of the C-terminal activated aryl thioester with the N-terminal cysteine, giving the native peptide bond (left, lower quarter). After purification of the native folded cyclotide, the product is analyzed by analytical quality control by reversed-phase high-performance liquid chromatography (HPLC) and matrix-assisted laser desorption ionization time-of-flight (MALDI-TOF) mass spectrometry (MS) (left, upper quarter). The native folded peptide is shown as Ribbon cartoon and the Cysteine connectivity as well as the full-length sequence of T20K is provided below (right, upper quarter).

cyclotide T20K on ALK-positive as well as ALK-negative malignant cells. Again T20K shows comparable results to the active cyclotides, including [G18K]-, [N29K]- and [G1K, T20K]kB1 by increasing the apoptotic and necrotic fraction compared to the inactive analogs. As a significant amount of preclinical data was available for T20K derived from other studies [21], we thus further focused on T20K and one inactive analog to characterize the impact of kalata-type cyclotides on ALCL cells in more detail.

3.2. T20K does not affect interleukin-2 expression in malignant T-cells

Previously, T20K was described to reduce interleukin (IL)-2 expression, interleukin secretion as well as IL2-receptor expression levels in normal T-cells in an experimental autoimmune encephalomyelitis mouse model [20]. Accordingly, we determined the influence of

T20K on IL-2 secretion of lymphoma cell lines. The levels of IL-2 in the media of ALCL cells with and without T20K were low and sparsely detected (Fig. 3A) and did not decrease upon treatment with T20K in concentrations of up to 4 μM. In contrast, treatment of the Burkitt-lymphoma B-cell line Ramos with cyclotide resulted in a concentration-dependent decreased IL-2 secretion. The higher levels of cytokine secretion without cyclotide addition might partly be explained by the rather low expression of IL-2 receptor alpha (IL2Rα; CD25) in this B-cell line in comparison to T-cells [24].

To verify the limited effects of T20K on IL-2 secretion, the T-cell leukemia cell line Jurkat E6.1 was deployed, which produces high amounts of IL-2 upon stimulation with phorbol esters. T-cell activation, mediated by stimulation with either IL-2, PMA and ionomycin, or a combination of them together with T20K, resulted in minor stimulation of the observed IL-2 secretion in the ALCL cell line SR786. In contrast,

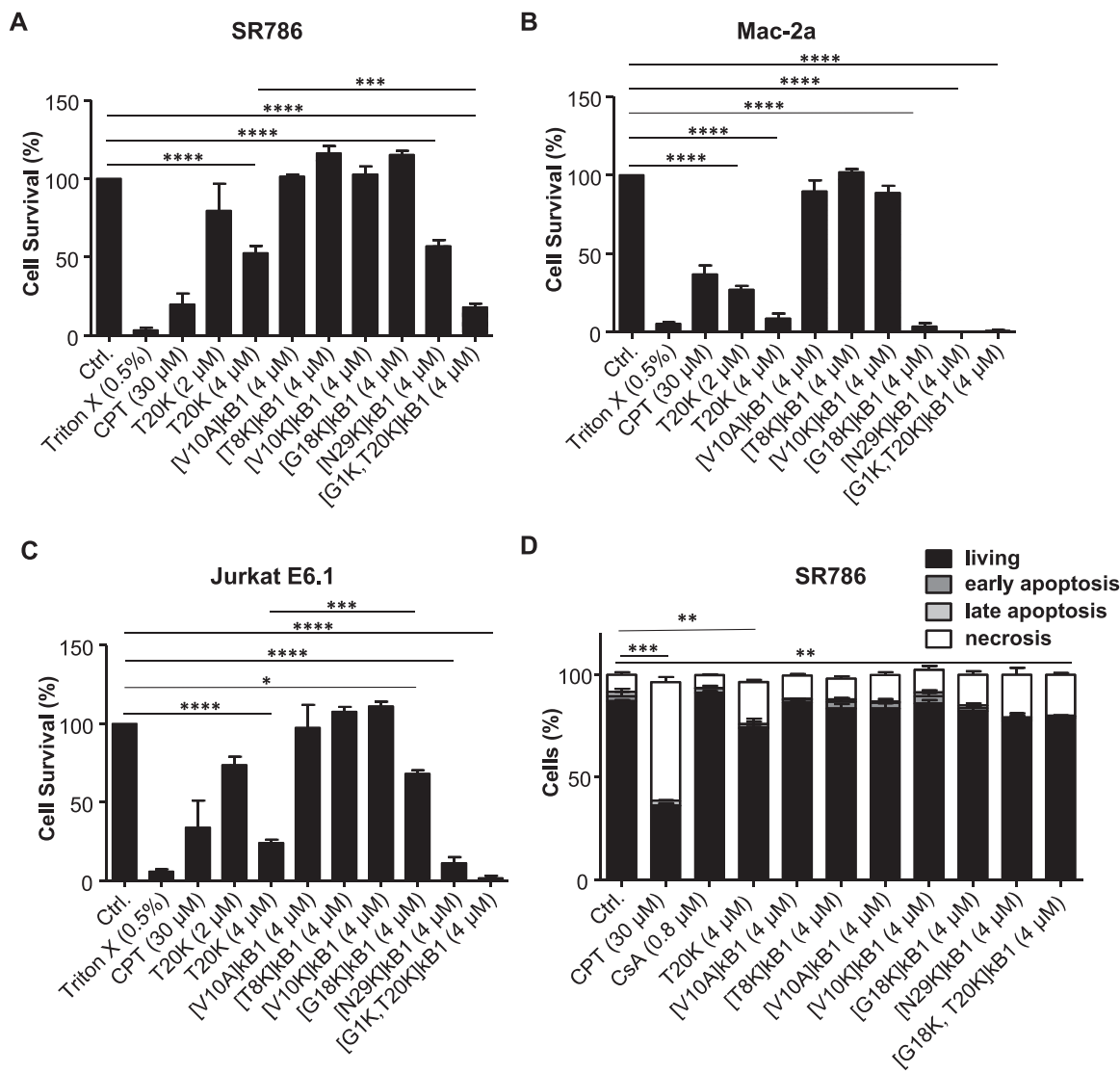


Fig. 2. Impaired cell viability of cyclotide-treated cells. (A–C) Cell viability assay of the ALK-positive ALCL cell line SR786, the ALK-negative ALCL cell line Mac-2a, and the T-cell leukemia cell line Jurkat E6.1. The cells were treated with Triton-X (0.5%), CPT (30 μM) or cyclotides in indicated concentrations for 24 h and cell viability was determined. Data are presented as mean ± SEM, n = 3 for [G18K]-, [N29K]-[G1K, T20K]-, [T8K]-, [V10K]- kB1; n > 3 for [V10A]kB1 and T20K. (D) Effects of cyclotide mutants on viability, apoptosis and necrosis of SR786 cells. The influence of PBS, CPT (30 μM), CsA (0.8 μM) or different cyclotides (4 μM) on viability was measured by flow cytometry after 24 h treatment using Annexin-V/7AAD staining. Data are presented as mean ± SEM of three independent experiments. Levels of significance were calculated using One-way ANOVA with subsequent Bonferroni posttest and shown for all inter-comparisons of Ctrl., T20K-, [G18K]-, [N29K]- and [G1K, T20K]-kB1 (A–D). *p < .05; **p < .01; ***p < .001; ****p < .0001.

the stimulation of the cell line Jurkat E6.1 resulted in highly increased IL-2 secretion compared to the unstimulated control. However, irrespective of the cell line and the activation stimulus tested in our experiments, the cytokine secretion remained unaltered upon T20K treatment (Fig. 3B). In contrast to previous reports on activated T-cells, the levels of CD25 expression did not decrease in ALCL cell lines when treated with either T20K or the negative control analog [V10A]kB1 for 24 h (Fig. 3C). The leukemic B-cell line Daudi was used as a negative control for CD25 expression. These data show that T20K treatment does not affect IL-2 induced growth stimuli of transformed T-cells.

3.3. T20K induces DNA double strand breaks

Based on the above-described results, T20K induces apoptosis of malignant T cell lines but does not interfere with IL-2 secretion. To analyze the apoptotic phenotype in more detail we analyzed the IC₅₀ levels for the representative cell line SR786 with T20K concentrations in the range of 2–14 μM (Suppl. Fig. 3). Using a panel of ALK-positive and

-negative ALCL and control cell lines, cell viability was determined using the CCK-8 cytotoxicity assay (Fig. 4A). To confirm the effectivity of the treatment, T20K in standard concentration of 4 μM (which is close to half maximum concentration as observed for SR786 cells) was directly compared with a negative control, the inactive analog [V10A]kB1. T20K led to a reduction in cell survival in the range of 10–80%, while [V10A]kB1 had no significant effect on survival of any of the tested cell lines.

In addition, the effect of the cyclotides on proliferation was investigated with the cell proliferation dye eFluor™ 670. SR786 cells were labeled with eFluor™ 670 and immediately seeded for treatment with T20K, [V10A]kB1 and control. Mean fluorescence intensity (MFI) of eFluor™ 670 has been determined before and after treatment for four days. Cells cultured with T20K showed a significantly lower reduction of the MFI indicating a proliferative disadvantage (Fig. 4B). After 4 days of treatment cells treated with the T20K peptide showed still double the amount of eFluor™ 670 compared to the inactive analog [V10A]kB1 and more or less triple the amount compared to control cells.

Another well-known indicator for apoptotic signaling induced by

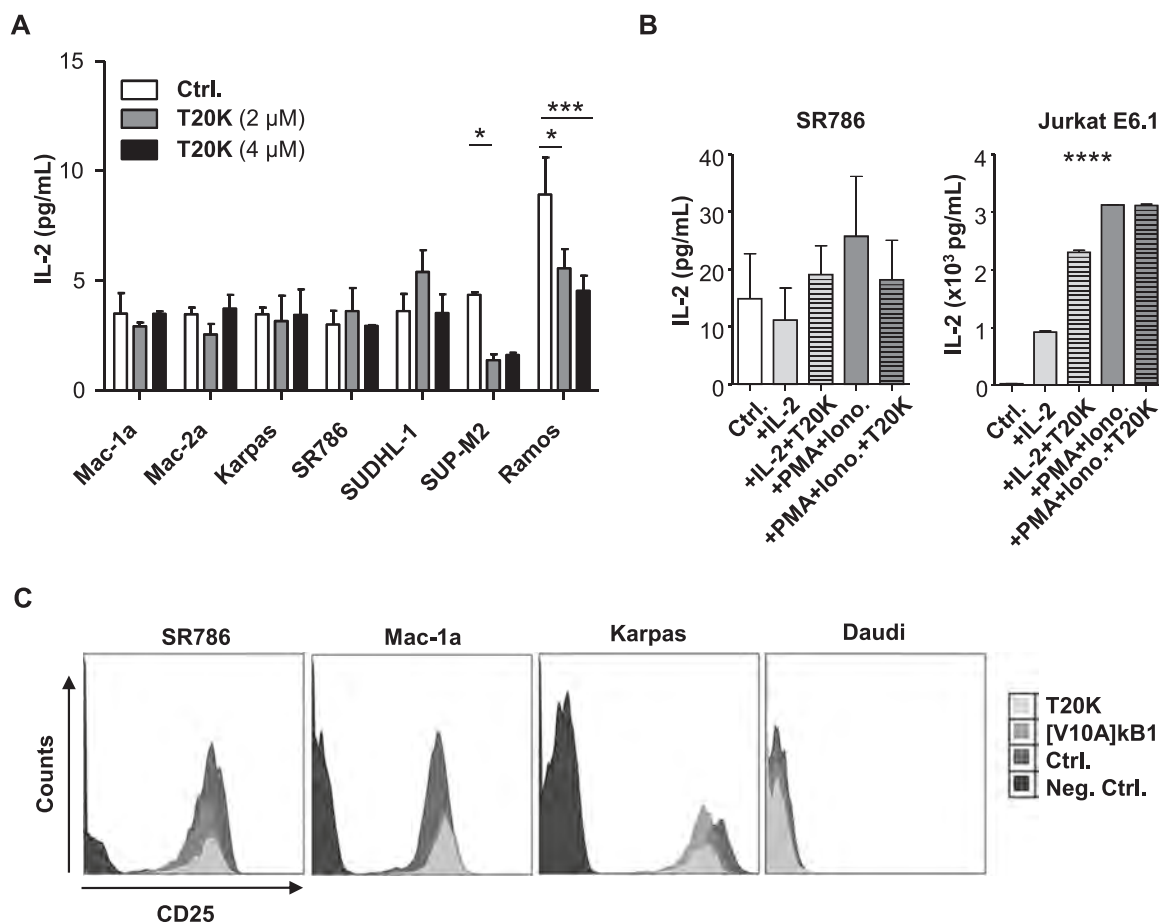


Fig. 3. Unaltered IL-2 production of lymphoma cell lines upon T20K treatment. (A) Indicated lymphoma cell lines were treated for 24 h with T20K at concentrations of 2 and 4 μM and IL-2 secretion measured by ELISA. Data are represented as mean \pm SD of three independent experiments. (B) Effects on IL-2 secretion of T-cell leukemia cell line Jurkat E6.1 and ALCL cell line SR786 after stimulation with IL-2 (2.5 ng/ml) or stimulation with PMA (50 ng/ml) in combination with ionomycin (500 ng/ml) with or without cyclotide T20K (4 μM) treatment for 2 h following restimulation with mitogens and further cultivation for 72 h. Data are presented as mean \pm SD of three independent experiments. (C) Different ALCL cell lines and a control were treated with T20K or the inactive variant V10A for 24 h and CD25 expression measured by flow cytometry of three independent experiments. Levels of significance were calculated using Two-way ANOVA with subsequent Bonferroni posttest for each cell line (A) and One-way ANOVA with subsequent Bonferroni posttest (B). * $p < .05$; ** $p < .001$; *** $p < .0001$.

cytotoxic agents, is the phosphorylation of $\gamma\text{-H2A.X}$. DNA double strand breaks induce cell cycle arrest and the phosphorylation of $\gamma\text{-H2A.X}$ is an early step in recruitment of DNA repair proteins. [25,26]. Hence, the level of $\gamma\text{-H2A.X}$ (Ser139) phosphorylation was examined upon T20K treatment of SR786 cells by flow cytometry. A significant increase (p-value: $<.0001$) in phosphorylation of $\gamma\text{-H2A.X}$ for T20K-treated cells (mean: 17.67%) in comparison to untreated cells (mean: 3.06%) was detected (Fig. 4C and Suppl. Fig. 4A). This increase in phosphorylation of $\gamma\text{-H2A.X}$ upon T20K treatment was validated in Mac-2a cells (Suppl. Fig. 4B), further affirming the apoptotic properties of the cyclotide.

3.4. The cyclotide T20K reduces tumor development in a xenotransplantation model

To evaluate the impact of T20K on human ALCL cell lines in vivo, transplantation of tumor cells into immunocompromised mice followed by cyclotide treatment was performed. Mice were subcutaneously injected with the ALK-positive cell line SR786 and the animals were treated three times per week with 1 mg/kg T20K in PBS or with pure PBS as a single *i.p.* administration per day as described previously [21]. Fourteen animals were *s.c.* injected and treatment started immediately on the day of tumor cell transplantation. Tumor development was observed, tumor size measured and tumor weight determined when animals had to be sacrificed after the tumors had reached a size of not

larger than 2 cm^3 (Fig. 5A). Afterwards tumors were isolated and single cell suspension of the isolated cells analyzed for apoptosis using Annexin V staining as well as cell cycle progression using Propidium Iodide staining and flow cytometry as described above.

Monitoring of tumor development over time exhibited a significantly reduced tumor volume of $\sim 50\%$ for T20K-treated animals (Fig. 5B). At the terminal endpoint, day 21, the tumor weight was significantly smaller in T20K-treated animals (Fig. 5C).

3.5. T20K treatment efficiently increases apoptosis in vivo

In the context of cell cycle state, no significant difference was detected by flow cytometry (Fig. 5D) or by immunohistochemical staining for the proliferation marker Ki67 in tumors (Suppl. Fig. 5, p-value: .27). Apoptosis as well as necrosis in T20K-treated tumor-derived cells was increased in comparison to PBS-treated cells. In turn, the percentage of living cells significantly dropped in response to T20K treatment (p-value: .0061), whereas the late apoptotic and necrotic cells increased in T20K-treated versus PBS-treated cells (Fig. 5E).

In line with these findings, tumors treated with T20K show increased protein levels of the tumor suppressor p53 compared to controls (Fig. 5F). In addition, we determined expression levels of several pro- and anti-apoptotic genes as well as the signal transducers and activators of transcription (STATs). The JAK/STAT pathway is a commonly

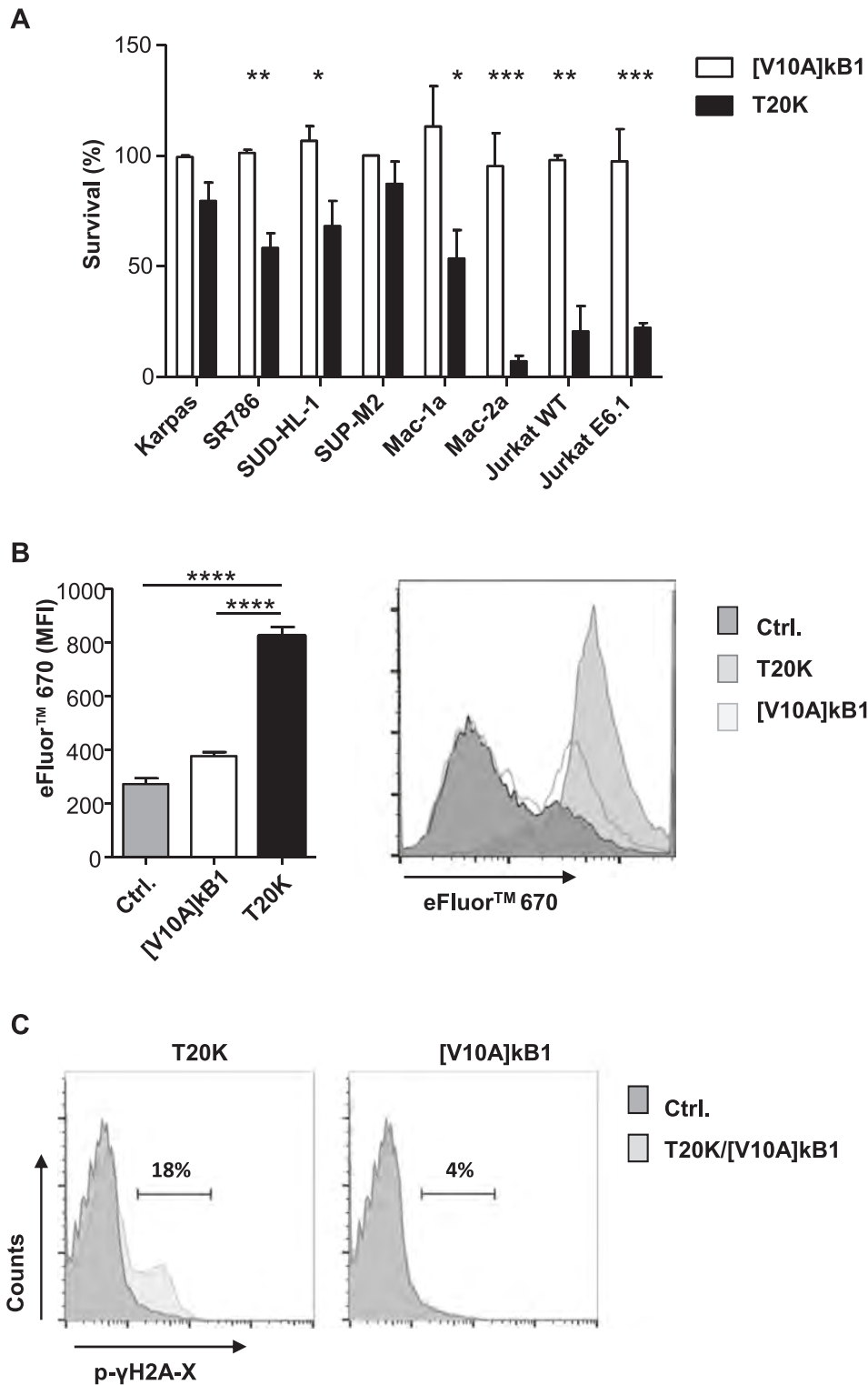


Fig. 4. Effects of cyclotides on survival, proliferation and DNA double strand breaks. (A) Cell survival of various ALK-positive (Karpas, SR786, SUD-HL-1, SUP-M2) and ALK-negative ALCL cell lines (Mac-1a, Mac-2a), and T-cell leukemia cell lines (Jurkat WT, Jurkat E6.1) using T20K (4 μM) or the inactive mutant [V10A]kB1 (4 μM) after 24 h treatment. Data are presented as mean ± SEM of three independent experiments. (B) Effects of cyclotides on the proliferation of ALK-positive SR786 cells was analyzed by the proliferation dye eFluor™ 670. Cells have been labeled and treated with either cyclotides at a concentration of 4 μM or control (ctrl) for 4 days. eFluor™ 670 MFI was analyzed after 4 days (left graph). A representative plot is shown (right). Data are presented as mean ± SEM of three independent experiments. (C) Influence of cyclotide treatment on SR786-cells after 24 h on cell cycle and apoptosis using p-γH2A.X staining. Cells were treated for 24–48 h with cyclotide at 4 μM concentration and analyzed by flow cytometry. Data are illustrated as representative plots of three independent experiments. Levels of significance were calculated using an unpaired t-test for [V10A]kB1 and T20K comparison for each cell line (A) and One-way ANOVA with subsequent Bonferroni posttest (B). *p < .05; **p < .01; ***p < .001; ****p < .0001.

deregulated pathway in hematologic malignancies and especially STATs are described to play an important role in ALCL. T20K treated tumors exhibited altered levels of *BCL-XL* and *MCL-1* compared to controls. The proto-oncogene *BCL-2* was not altered by T20K treatment. Interestingly, we detected significantly increased levels of *STAT5A* and a non-significant trend of downregulation in levels of *STAT3* in tumors from mice treated with T20K (Fig. 5G and Suppl. Fig. 6A and B). To validate the T20K-STAT5 axis determined *ex vivo* we treated SR786 cells with

T20K *in vitro* and analysed *STAT5A* mRNA levels by qPCR and total *STAT5* protein levels by intracellular FACS stainings (Suppl. Fig. 6C and D). In line, mRNA as well as protein levels of *STAT5* increased with T20K treatment.

In summary, T20K treatment *in vivo* results in reduced tumor mass and increased apoptosis linked to enhanced p53 and *STAT5A* expression levels.

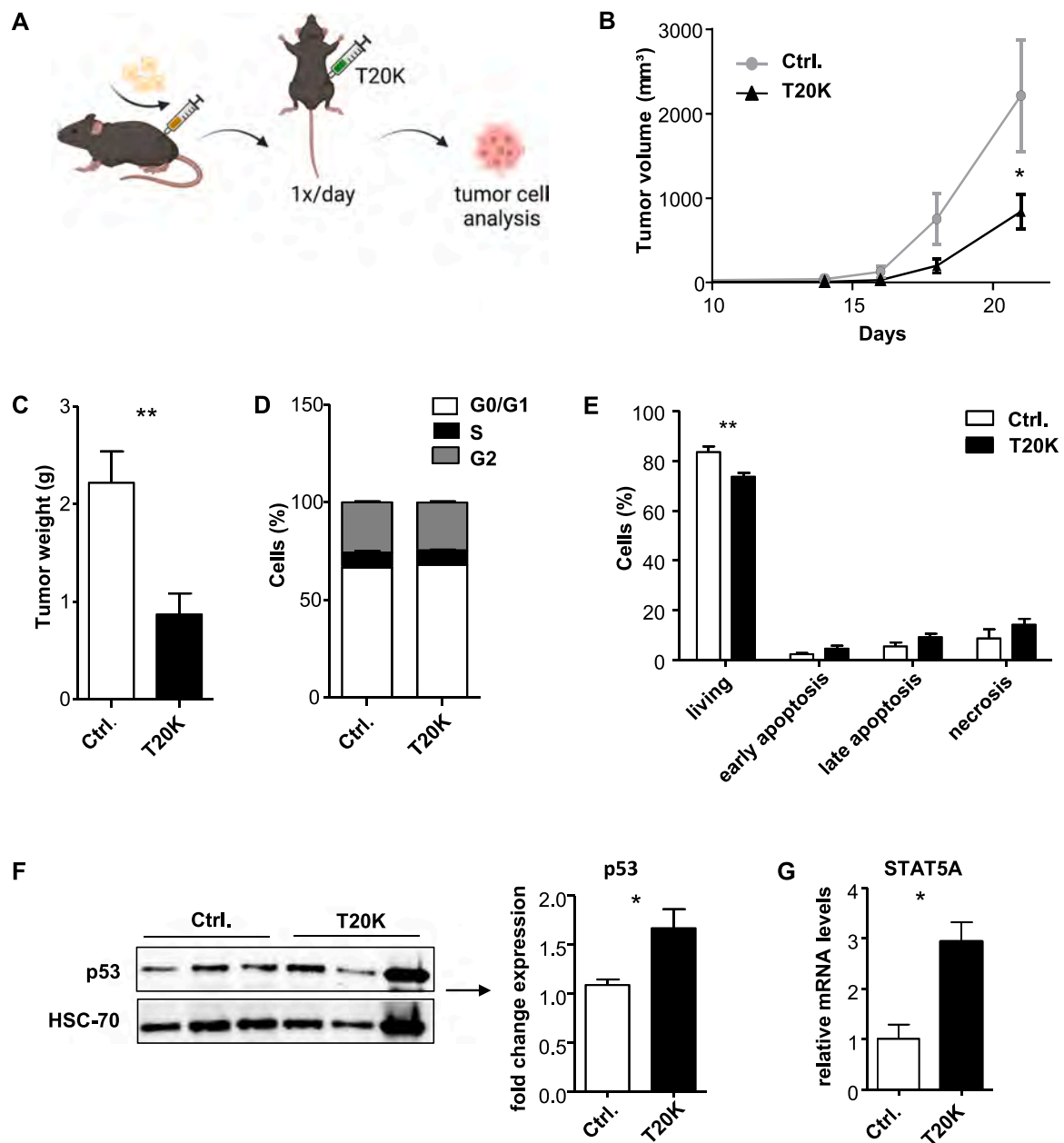


Fig. 5. T20K leads to reduction in tumor volume in vivo. (A) 0.75×10^6 SR786 cells were injected s.c. and mice were treated immediately with 1 mg/kg T20K i.p. or PBS i.p. 3-times per week. (B) Tumor volume was analyzed over time (PBS: n = 4; T20K: n = 6). (C) Bar graph represents tumor weight of mice treated with PBS or T20K on day 21 after injection (PBS: n = 4; T20K: n = 6). (D) Cell cycle profiles on tumor cells isolated from T20K-treated versus PBS-treated mice measured by flow cytometry. Bar charts represent summarized data of T20K-treated and control (PBS) mice (PBS: n = 4; T20K: n = 9). (E) Effect of cyclotide treatment on apoptosis and necrosis in tumors of T20K-treated and PBS-treated mice (PBS: n = 3; T20K: n = 3). (F) Tumor samples were analyzed for p53 protein levels by Western blot. Expression levels were quantified in comparison to housekeeping gene by ImageJ (n = 3/group). (G) Cells derived from T20K- and PBS-treated tumors analyzed for relative STAT5A mRNA expression (PBS: n = 3; T20K: n = 9). Fold change (mean \pm SEM) normalized to GAPDH. Levels of significance were calculated using an unpaired t-test (C–G). *p < .05; **p < .01.

4. Discussion

In recent years the library of plant-derived cyclic peptides vastly increased revealing a large repertoire of sequence and structural diversity, and estimates suggest that we only discovered a small fraction of all available cyclotides in the plant kingdom [27,28]. The cyclotide kalata B1 has been previously described for its anti-proliferative effects on T cells [20,21], and the lysine-mutated cyclotide T20K was shown to be very potent in a mouse model of multiple sclerosis [21]. In this pioneering study we determined the activity of T20K in the context of T-cell lymphoma. An effective induction of apoptosis of various ALCL cell lines

could be demonstrated in vitro by treatment with T20K. The mutants [G18K]-, [N29K]- and [G1K, T20K]kB1, which carry amino acid replacements at the amendable face of the peptide, are active variants of kalata B1 and showed similar effects on survival as the lead peptide T20K [20]. In contrast, the mutants [T8K]-, [V10A]-, [V10K]kB1 did not affect cell survival, as they contain changes in amino acid positions of the bioactive face of the peptide [21]. In addition, a tumor suppressive potential of T20K was demonstrated in vivo using xenotransplantation of ALCL cells into mice. The cyclotide treatment resulted in a significant ~50% reduction of the tumor volume and increased apoptotic and necrotic signaling in the tumor cells compared to controls.

By the detection of pro- and anti-apoptotic mediators we gained insight into T20K's role on intracellular signaling. The importance of STATs is exemplified by NPM-ALK-driven hematopoietic malignancies [29,30]. In such tumors driven by NPM-ALK, STAT3 makes a significant contribution to the pathogenesis at all stages of the disease [31–33]. The development of therapeutic strategies to target STAT proteins has met with limited success [34], therefore therapies leading to deregulated STAT levels are of high potential to bring benefit for patients [28–30]. Thus, the slight decrease of STAT3 as well as the anti-apoptotic mediator *BCL-XL* in T20K treated tumor cells further demonstrate the feasibility of T20K treatment. Interestingly, *STAT5A* expression levels are significantly increased upon cyclotide treatment. So far, in ALCL contradictory findings on the role of STAT5 were reported in the literature, impeding a clear interpretation of the role for this protein. For instance, it was observed in NPM-ALK positive cell lines that *STAT5A* expression is inhibited via an NPM-ALK induced methylation by STAT3 [35]. In addition, in ALK-positive ALCL, it was found that *STAT5B* gets activated via the NPM-ALK kinase resulting in increased cell growth and survival [31]. A recent study in BCR-ABL driven leukemia points as well to the divergent functions of *STAT5A* and *STAT5B*, which needs to be further analyzed in different diseases [36]. In line with our data of enhanced p- γ -H2A.X and increased *STAT5A* levels upon T20K treatment, other studies describe a role for *STAT5A* to induce DNA-double strand breaks through increased reactive-oxygen species (ROS) production. This process is linked to p53 induced senescence in fibroblasts [37]. In BCR-ABL driven diseases this process is explained to be part of a feed-forward loop accelerating disease progression, in which BCR-ABL1 enhances its own mutation rate in a *STAT5*-ROS dependent manner [38].

T20K has been found inside the cell ([39,40] unpublished data) but still little is known about the intracellular effects of cyclotides, but for example the cyclotide vigno 5 (isolated from *Viola ignobilis*) has been shown to activate the intrinsic pathway of apoptosis via cytochrome C release and caspase 9 activation [41]. Further studies are therefore needed to clarify the mediated intrinsic cellular responses upon cyclotide treatment in ALCL [42–44].

In line with the previous results showing that the cyclotide T20K has a high anti-proliferative effect on T-cell mediated autoimmune diseases, we demonstrate in this study that T20K has a similar influence on the proliferation of the transformed T-cells. However, this proliferative alteration was more drastic in the in vitro situation. Unexpectedly, the transformed T-cells did not react with a different IL-2 production in response to T20K treatment contradictory to primary T-cells. The potential use of this cyclotide for treatment of ALCL patients might form the baseline for forthcoming drug development and detailed preclinical assessment. In upcoming studies, the structural stability of the cyclotides should be taken under consideration, as they are remarkably resistant against enzymatic, chemical and thermal degradation rendering them orally active [14]. These properties could validate to explore the use of cyclotides as therapeutic option in ALCL. At the very least, our results contribute another important example about the biological activity of cyclotides, an important class of nature-derived peptides with applications in drug discovery and development.

CRediT authorship contribution statement

J.L., P.K., H.P.M., J.G. and S.E. performed in vitro and in vivo experiments using the different cyclotides. R.H. performed peptide synthesis, purification and analysis. K.T. supported experiments. J.L., C.W.G., R.H. and K.K. prepared the Figures. All authors analyzed the data. C.W.G., D.S. and K.K. designed experiments. J.L., C.W.G., D.S. and K.K. wrote the manuscript.

Conflict of interest statement

C.W.G. is scientific advisor of Cyxone AB. The other authors declare no competing financial interests.

Acknowledgements

This research was supported by a grant from the Austria Wirtschaftsservice GmbH (AWS) Prize-P1621670 (to C.W.G. as principal investigator and D.S. and K.K. as co-investigators).

Appendix A. Supporting information

Supplementary data associated with this article can be found in the online version at doi:10.1016/j.biopha.2022.113486.

References

- [1] E. Mereu, E. Pellegrino, I. Scarfo, G. Inghirami, R. Pivia, The heterogeneous landscape of ALK negative ALCL, *Oncotarget* 8 (2017), 18525–1853.
- [2] G. Hapgood, K.J. Savage, The biology and management of systemic anaplastic large cell lymphoma, *Blood* 26 (2015) 17–25.
- [3] J. Vose, J. Armitage, D. Weisenburger, International peripheral T-cell and natural killer/T-cell lymphoma study: pathology findings and clinical outcomes, *J. Clin. Oncol.* 26 (2008) 4124–4130.
- [4] M.C. Kinney, R.A. Higgins, E.A. Medina, Anaplastic large cell lymphoma: twenty-five years of discovery, *Arch. Pathol. Lab. Med.* 135 (2011) 19–43.
- [5] I. Vivanco, C.L. Sawyers, The phosphatidylinositol 3-Kinase AKT pathway in human cancer, *Nat. Rev. Cancer* 2 (2002) 489–501.
- [6] J.V. Alvarez, D.A. Frank, Genome wide analysis of STAT target genes: elucidating the mechanism of STAT-mediated oncogenesis, *Cancer Biol. Ther.* 3 (2004) 1045–1050.
- [7] D.J. Newman, G.M. Cragg, Natural products as sources of new drugs from 1981 to 2014, *J. Nat. Prod.* 79 (2016) 629–661.
- [8] P.G. Arnison, M.J. Bibb, G. Bierbaum, A.A. Bowers, T.S. Bugni, Ribosomally synthesized and post-translationally modified peptide natural products: overview and recommendations for a universal nomenclature, *Nat. Prod. Rep.* 30 (2013) 108–160.
- [9] C. Gründemann, J. Koebach, R. Huber, C.W. Gruber, Do plant cyclotides have a potential as immunosuppressant peptides, *J. Nat. Prod.* 75 (2012) 167–174.
- [10] D.J. Craik, N.L. Daly, T. Bond, C. Waine, Plant cyclotides: a unique family of cyclic and knotted proteins that defines the cyclic cystine knot structural motif, *J. Mol. Biol.* 294 (1999) 1327–1336.
- [11] M.L. Colgrave, D.J. Craik, Thermal, chemical, and enzymatic stability of the cyclotide kalata B1: the importance of the cyclic cystine knot, *Biochemistry* 43 (2004) 5965–5975.
- [12] C.W. Gruber, M. O'Brien, Uterotonic plants and their bioactive constituents, *Planta Med.* 77 (2011) 207–220.
- [13] L. Gran, Oxytocic principles of *Oldenlandia affinis*, *Lloydia* 36 (1973) 174–178.
- [14] R. Burman, J. Svedlund, J. Feith, S. Hassan, A. Hermann, R.J. Clark, et al., Evaluation of toxicity and antitumor activity of cycloviolacin O2 in mice, *Pept. Sci.* 94 (2010) 629–634.
- [15] S.L. Gerlach, R. Rathinakumar, G. Chakravarty, U. Göransson, W.C. Wimley, S. P. Darwin, et al., Anticancer and chemosensitizing abilities of cycloviolacin O2 from *Viola odorata* and psyle cyclotides from *Psychotria leptothyrsa*, *Biopolymers* 94 (2010) 617–625.
- [16] A. Herrmann, R. Burman, J.S. Mylne, G. Karlsson, J. Gullbo, D.J. Craik, et al., The alpine violet, *Viola biflora*, is a rich source of cyclotides with potent cytotoxicity, *Phytochemistry* 69 (2008) 939–952.
- [17] R. Hellinger, J. Koebach, H. Fedchuk, B. Sauer, R. Huber, C.W. Gruber, et al., Immunosuppressive activity of an aqueous *Viola tricolor* herbal extract, *J. Ethnopharmacol.* 151 (2014) 299–306.
- [18] L. Gran, On the effect of a polypeptide isolated from 'Kalata-Kalata' (*Oldenlandia affinis* DC) on the oestrogen dominated uterus, *Acta Pharmacol. Toxicol.* 33 (1973) 400–408.
- [19] R. Hellinger, J. Koebach, D.E. Soltis, E.J. Carpenter, G. Ka-Shu Wong, C. W. Gruber, Peptidomics of circular cysteine-rich plant peptides: analysis of the diversity of cyclotides from *Viola tricolor* by transcriptome and proteome mining, *J. Proteome Res.* 14 (11) (2015) 4851–4862.
- [20] C. Gründemann, K. Thell, K. Lengen, M. Garcia-Käufer, Y.H. Huang, R. Huber, et al., Cyclotides suppress human T-lymphocyte proliferation by an interleukin 2-dependent mechanism, *PLoS One* 8 (2013), e68016, <https://doi.org/10.1371/journal.pone.0068016>.
- [21] K. Thell, R. Hellinger, E. Sahin, P. Michenthaler, M. Gold-Binder, T. Haider, et al., Oral activity of a nature-derived cyclic peptide for the treatment of multiple sclerosis, *Proc. Natl. Acad. Sci. USA* 113 (2016) 3960–3965.
- [22] C. Gründemann, K.G. Stenberg, C.W. Gruber, *Int. J. Pept. Res. Ther.* (2018), <https://doi.org/10.1007/s10989-018-9701-1>.
- [23] P. Keov, Z. Liutkeviciute, R. Hellinger, R.J. Clark, C.W. Gruber, Discovery of peptide probes to modulate oxytocin-type receptors of insects, *Sci. Rep.* 81 (2018) 10020.
- [24] M.J. Flynn, F. Zammarchi, P.C. Tyrer, A.U. Akarca, N. Janghra, C.E. Britten, et al., ADCT-301, a pyrrolizidine alkaloid (PBD) dimer-containing antibody–drug conjugate (ADC) targeting CD25-expressing hematological malignancies, *Mol. Cancer Ther.* 15 (2016) 2709–2721.
- [25] L.J. Kuo, L. Yang, Gamna-H2AX – a novel biomarker for DNA double-strand breaks, *Vivo* 22 (3) (2008) 305–309.

- [26] J. Yuan, R. Adamski, J. Chen, Focus on histone variant H2AX: to be or not to be, *FEBS Lett.* 584 (2010) 3717–3724.
- [27] C.W. Gruber, D.C. Elliott, P.G. Ireland, S. Delprete, U. Desein, D.J. Göransson, et al., Distribution and evolution of circular miniproteins in flowering plants, *Plant Cell Online* 20 (2018) 2471–2483.
- [28] R. Hellinger, J. Koehbach, D.E. Soltis, E.J. Carpenter, G. Ka-Shu Wong, C. W. Gruber, Peptidomics of Circular Cysteine-Rich plant peptides: analysis of the diversity of cyclotides from *Viola tricolor* by transcriptome and proteome mining, *J. Proteome Res.* 1411 (2015) 4851–4862.
- [29] T.A. Eyre, D. Khan, G.W. Hall, G.P. Collins, *Eur. J. Haematol.* 93 (2014) 455–468, <https://doi.org/10.1111/ejh.12360>.
- [30] R.Y. Bai, T. Ouyang, C. Miething, S.W. Morris, C. Peschel, J. Duyster, Nucleophosmin-anaplastic lymphoma kinase associated with anaplastic large-cell lymphoma activates the phosphatidylinositol 3-kinase/Akt antiapoptotic signaling pathway, *Blood* 96 (2000) 4319–4327.
- [31] A. Buetti-Dinh, T. O'Hare, R. Friedman, Sensitivity analysis of the NPM-ALK signalling network reveals important pathways for anaplastic large cell lymphoma combination therapy, *PLoS One* 11 (2016), e0163011.
- [32] R. Chiarle, W.J. Simmons, H. Cai, G. Dhall, A. Zamo, R. Raz, et al., Stat3 is required for ALK-mediated lymphomagenesis and provides a possible therapeutic target, *Nat. Med.* 11 (2005) 623–629.
- [33] A. Zamo, R. Chiarle, R. Piva, J. Howes, Y. Fan, M. Chilosi, et al., Anaplastic lymphoma kinase (ALK) activates Stat3 and protects hematopoietic cells from cell death, *Oncogene* 21 (2002) 1038–1047.
- [34] J.S. Abramson, T. Feldman, A.R. Kroll-Desrosiers, L.S. Muffly, E. Winer, C. R. Flowers, et al., Peripheral T-cell lymphomas in a large US multicenter cohort: prognostication in the modern era including impact of frontline therapy, *Ann. Oncol.* 25 (2014) 2211–2217.
- [35] Q. Zhang, H.Y. Wang, X. Liu, M.A. Wasik, STAT5A is epigenetically silenced by the tyrosine kinase NPM1-ALK and acts as a tumor suppressor by reciprocally inhibiting NPM1-ALK expression, *Nat. Med.* 13 (2007) 1341–1348.
- [36] F. Belutti, A.S. Tigan, S. Nebenfuhr, M. Dolezal, M. Zojer, R. Grausenburger, et al., CDK6 antagonizes p53-induced responses during tumorigenesis, *Cancer Discov.* 87 (2018) 884–897.
- [37] F.A. Mallette, O. Moiseeva, V. Calabrese, B. Mao, M.F. Gaumont-Leclerc, G. Ferbeyre, Transcriptome analysis and tumor suppressor requirements of STAT5-induced senescence, *Ann. N. Y. Acad. Sci.* 1197 (2010) 142–151.
- [38] W. Warsch, E. Grundschober, A. Berger, L. Gille, S. Cerny-Reiterer, A.S. Tigan, et al., STAT5 triggers BCR-ABL1 mutation by mediating ROS production in chronic myeloid leukaemia, *Oncotarget* 3 (2012) 1669–1687.
- [39] S.T. Henriques, Y.H. Huang, S. Chaouis, M.A. Sani, A.G. Poth, F. Separovic, et al., The prototypic cyclotide kalata B1 has a unique mechanism of entering cells, *Chem. Biol.* 22 (2015) 1087–1097.
- [40] R. Hellinger, E. Muratspahić, S. Devi, J. Koehbach, M. Vasileva, P.J. Harvey, et al., Importance of the cyclic cystine knot structural motif for immunosuppressive effects of cyclotides, *ACS Chem. Biol.* 6 (2021) 2373–2386.
- [41] M.A. Esmaili, N. Abagheri-Mahabadi, H. Hashempour, M. Farhadpour, C. W. Gruber, A. Ghassempour, *Viola plant cyclotide vigno 5 induces mitochondria-mediated apoptosis via cytochrome C release and caspase activation in cervical cancer cells*, *Fitoterapia* 109 (2016) 162–168.
- [42] Y.H. Huang, M.L. Colgrave, N.L. Daly, A. Keleshian, B. Martinac, D.J. Craik, The biological activity of the prototypic cyclotide kalata B1 is modulated by the formation of multimeric pores, *J. Biol. Chem.* 284 (2009) 20699–20707.
- [43] S.T. Henriques, Y.H. Huang, K.J. Rosengren, H.G. Franquelim, F.A. Carvalho, A. Johnson, et al., Decoding the membrane activity of the cyclotide kalata B1: the importance of phosphatidylethanolamine phospholipids and lipid organization on hemolytic and anti-HIV activities, *J. Biol. Chem.* 286 (2011) 24231–24241.
- [44] I.M. Torcato, Y.H. Huang, H.G. Franquelim, D.D. Gaspar, D.J. Craik, M.A.R. B. Castanho, et al., The antimicrobial activity of Sub3 is dependent on membrane binding and cell-penetrating ability, *ChemBioChem* 14 (2013) 2013–2022.